

Onset of Forming Ordering in Uniaxially Stretched Poly(ethylene terephthalate) Films Due to $\pi-\pi$ Interaction Clarified by the Fluorescence Technique

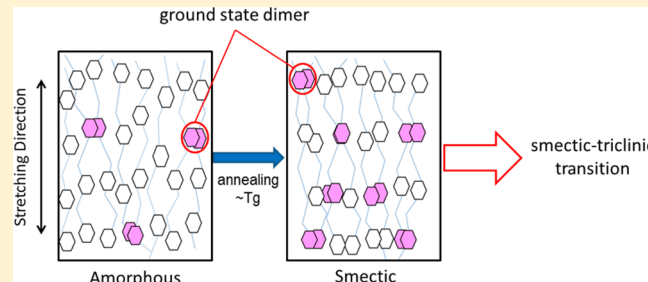
Tomohiro Sago,[†] Hideyuki Itagaki,^{*,†,‡} and Tsutomu Asano[§]

[†]Department of Chemistry, Graduate School of Science and Technology, Shizuoka University, 836 Ohya, Suruga-ku, Shizuoka 422-8529, Japan

[‡]Department of Chemistry, School of Education, Shizuoka University, 836 Ohya, Suruga-ku, Shizuoka 422-8529, Japan

[§]Center for Instrumental Analysis, Shizuoka University, 836 Ohya, Suruga-ku, Shizuoka 422-8529, Japan

ABSTRACT: The initial stage of a cold crystallization process for uniaxially stretched poly(ethylene terephthalate) (PET) was examined in detail by means of fluorescence spectroscopy and wide-angle X-ray diffraction measurements. The cold crystallization of PET annealed at around T_g , which occurred by way of mesomorphic ordering, was investigated with respect to the $\pi-\pi$ interactions between the main-chain phenylene groups of PET by measuring the polarized fluorescence intensities and the distribution of the ground-state dimer (GD) of PET. The mesomorphic ordering was found to be induced by GDs acting as nucleation centers; these GDs seemed to progressively assume a smectic form upon annealing at temperatures around T_g . Moreover, the flat plane in the smectic form was suggested as the cause of the unique tilted orientation observed in triclinic PET crystals.



INTRODUCTION

It is well-known that poly(ethylene terephthalate) (PET) solidifies in the form of an amorphous glass when quenched from the melt.^{1,2} Zachmann et al. studied the primary crystallization of PET from a morphological standpoint.^{3–6} When PET is drawn above the glass transition temperature (T_g), Bonart first reported the occurrence of a paracrystalline structure;⁷ the structure of PET varied during the drawing treatment from a totally amorphous to a nematic and finally to a smectic state. From electron microscopic observations, Yeh and Geil pointed out that glassy PET is composed of ball-like structures in which PET molecules exhibit a paracrystalline order.^{8,9} According to them, strain-induced crystallization can be explained by rotation, alignment, and optimization of the internal order of the paracrystalline ball-like structures. Triclinic PET crystalline phase sometimes reveals a unique tilted orientation in the $\bar{z}30$ plane, which was first studied by Daubeny et al.¹⁰ Asano and Seto later analyzed in detail the dependence of the molecular tilted orientation on the annealing temperature.¹¹ They found the sharp meridional reflection in the beginning of the crystallization having spacing of 1.03 nm and proposed the existence of a monoclinic paracrystalline structure in the early stages of crystallization from an oriented glass. Considering the transition from the paracrystalline to the triclinic structure, they succeeded to explain the variation of the tilted orientation depending on the annealing temperature.¹¹ At a periodicity of approximately 1.03 nm, another interpretation was reported using Fourier transform calculations of isolated-

chain models.^{12,13} Conformations of monomeric units, with some or all of these conformations exhibiting calculated minima of conformational energy, could be randomly joined together at low energy cost, giving rise to highly extended conformationally disordered PET chains with an average periodicity close to 1.03 nm. However, Asano et al. examined the structural changes that take place in PET films when amorphous PET films that have been drawn at temperatures near T_g are annealed at different temperatures (50–240 °C) for different annealing times (10–10⁴ s).¹⁴ The X-ray scattering results have revealed the emergence of smectic ordering at 60 °C with a period of 1.07 nm. At 70 °C, a layer structure on the scale of 11 nm emerged, and finally, triclinic ordering began to be observable above 80 °C. The appearance of the layer structure prior to the development of triclinic crystals was found to be associated with a density difference along the molecular direction produced by a molecular tilting mechanism. After the work by Asano et al.,¹⁴ the mechanism for the cold crystallization of PET by way of mesomorphic or smectic ordering has been established by quite a few papers that support the concept.^{15–20} Keum et al. studied the transient structure of cold-drawn PET and found the appearance of the smectic peak having 1.04 nm at lower than the glass transition temperature without annealing.¹⁵ Kim et al. investigated structure development in

Received: August 30, 2013

Revised: December 6, 2013

Published: December 12, 2013

the continuous laser-drawing process and observed the 001' reflection from 0.16 ms after the necking.¹⁶ By means of in-situ synchrotron SAXS and WAXD, Kawakami et al. found that the deformation-induced transitions developed through several zones having nematic, smectic C, and smectic A orders.¹⁸ Mahendrasingam et al. studied several types of drawing mechanism using synchrotron radiation and observed nearly the same results by Asano et al. They found the smectic C reflection at 35 °C.¹⁹ These results suggest that the mesomorphic phase appears rapidly after the drawing, which develops depending on heat treatments. However, there is still one question that remains unsolved, which is "what is the origin of the mesomorphic ordering?" The goal of the present paper is to search for this cause.

We have applied fluorescence technique to clarify this cause in addition to the X-ray analysis because the interaction between phenylene rings of PET main chains can be directly monitored by this technique. PET has a fluorescent phenylene moiety in the main chain showing its fluorescence peak at 330–340 nm in fluid solution, but fluorescence with fine structures at 369 and 387 nm observed only for thick PET films have been assigned to the phenylene ground-state dimer (GD),^{21–23} which has an absorption peak at 336 nm. The intrinsic luminescence of PET films was not well characterized until we studied PET films prepared by a spin-casting method, which provides the most reproducible conditions to prepare films.^{24,25} Finally, we found that PET and poly(1,4-butylene terephthalate) (PBT) fluorescence consist of two fluorescent components in addition to the GD: one with a peak near 330 nm coming out from the main-chain phenylene groups in the crystalline region and the other at longer wavelengths from the phenylene in the amorphous region.^{24–26} We have succeeded to study on the dynamic processes of cold crystallization taking place in thin films of PET²⁷ and PBT²⁸ by monitoring these fluorescence intensities.

Here is another powerful tool to monitor the orientation of phenylene groups of PET in the mesomorphic order. That is the method of measuring polarized fluorescence intensities by rotating a sample around the excitation light, namely PFR method. We have applied the PFR method to various samples having fluorescent groups and molecules and obtained precious findings for years; the determination of three-dimensional arrangement of guest naphthalene (NP) in highly oriented syndiotactic polystyrene (SPS) films with SPS/NP cocrystals,²⁹ orientation of atactic polystyrene chains and the free volume among them when stretched uniaxially,³⁰ orientation of the amorphous or mesomorphic phases of SPS stretched films when they are exposed to NP gas,³¹ or the detection of highly oriented guest molecule in SPS films containing a fluorescent coumarin derivative.³² We have tried to generalize the PFR method as structural analysis such as orientation and/or distributions of oriented structure by applying the method to samples having highly to poorly ordered structures. However, all these studies have been confined with those using fluorescence of small molecules added into the system. We need to show that the PFR method is useful for knowing distributions of ordered structure by measuring directly the fluorescence reflecting polymer chain itself. Thus, we have applied the PFR method to aromatic polyester with fluorescent groups in its main chain in order to observe directly structural change of polymer main chain without adding any probe molecules in the present paper.

No other papers have ever applied the PFR method to PET films for probing the orientation of main chain. We have found that the distributions of GD vary with drawing ratios and/or annealing temperatures. Using PFR, we report a strong evidence of an onset mechanism of ordering formation during annealing process of uniaxially drawn PET. The unique tilted orientation of PET is also explained by an effect of the flat smectic plane.

EXPERIMENTAL SECTION

Materials. The PET sample used for this work was purchased from Aldrich Co. (inherent viscosity = 0.59 dL/g). All the PET films were first prepared by melting polymer pellets at 280 °C for 7 min, compressing them at 20 MPa for 5 min, and then quenching them quickly in ice water. The films were dried for more than 24 h under vacuum at 40 °C. Each 5 × 1 cm PET film was obtained by die-cutting. The samples were stretched uniaxially at set drawing ratios by a manual stretching machine at a deformation rate of ~4.4% s⁻¹ in hot water whose temperature was kept constant between 67 and 80 °C. T_g of the PET films was measured to be 71 °C. After the stretching, PET films were dried under vacuum for 3 days at 40 °C. Annealing of PET films was carried out at each constant temperature under vacuum for 24 h. Stretched PET films were fixed with a metallic binder in order to keep drawing ratios constant during being annealed. A part of the film was cut and used for the measurements; then the rest of the film was again fixed with a metallic binder and annealed at higher temperatures. Thus, all the measurements (WAXD, SAXS, and PFR) were carried out for the same film annealed at a temperature. The thicknesses of PET films as received, after stretching, and after annealing with a metallic binder were ~220, 110, and 100 μm.

Measurements. Fluorescence depolarization was measured at 25 °C on a Hitachi F-4500 spectrofluorometer. Figure 1 demonstrates the

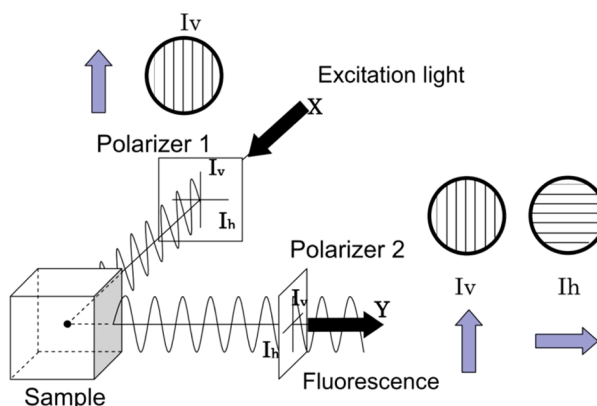


Figure 1. Sketch of polarized fluorescence measurements. Iv and Ih are unit vectors of electric field for the polarized light selected by a polarizer. Polarizer 1 is set as to choose a polarized light whose vector of electric field is Iv as the excitation light, while polarizer 2 is automatically set to be either parallel or vertical to polarizer 1.

general measurement of polarized fluorescence of samples. Two sets of polarizers are used: polarizer 1 is set as Iv shown in the figure and selects the polarized light whose vector of electric field is vertical to the direction of progress as the excitation light of a sample. The excitation light for the polarized fluorescence measurements is always the same as in Figure 1. The polarizer 2 is set in front of the detector as is shown by either Iv or Ih. The fluorescence intensity of a sample is defined to be I0 and I90 when polarizer 2 (fluorescence) is set as Iv and Ih, respectively. I0 and I90 are dependent on how much a sample absorbs the excitation light and how much its polarized fluorescence can go through the polarizer 2.

All the films were stuck on a holder with a circle hole whose diameter is 2.0 mm in order to irradiate the exact same part no matter

how the film was rotated. Fluorescence measurements of films were carried out by placing the films on a holder shown in Figure 2. Films

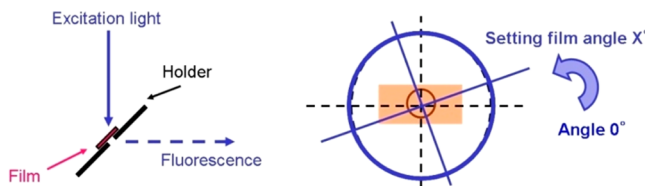


Figure 2. Setting way of a sample film for the measurements of polarized fluorescence together with the definition of setting film angle. The stretching direction is set to be 0° .

were rotated by every 10° in the same plane whose center was at 60° to the exciting beam. In particular, the stretching direction was defined to be 0° . To measure GD polarized fluorescence, a Hitachi automatic polarizer was attached to a Hitachi F-4500 spectrophotofluorometer. Excitation wavelength was 340 nm. The I_0 and I_{90} values were determined by averaging the polarized fluorescence intensities around peak (16 points) measured repeatedly: two or three times each for one angle from 0 to 360° and again from 360 to 0° . Thus, the I_0 and I_{90} values for one setting angle of a film are the average of at least 64 data. In general, fluorescence intensities are expressed in arbitrary units because they change as a function of the slit width of the excitation light, the emission light, the voltage of the detector, or any two or all three of these. The values of I_0 and I_{90} in the same figure were obtained under the same conditions as the measurements.

X-ray diffraction patterns were measured at room temperature using a Rigaku MicroMax7HFM, which was installed at Center for Instrumental Analysis of Shizuoka University, with a beam of $\text{Cu K}\alpha$ radiation ($\lambda = 0.15418 \text{ nm}$) that was finely focused by a confocal mirror and a collimator. The diffraction patterns of WAXD were detected by a Rigaku R-axisIV++ and recorded on an imaging plate. The data were analyzed by using the FIT2D program. Diffraction intensities at constant 2θ shown in a diffraction pattern were obtained by the integration of all the diffraction intensities around the beam.

Method of Measuring Polarized Fluorescence by Rotating Sample around the Excitation Light (PFR Method). For cases in which the transition moments for absorption and fluorescence of a chromophore or fluorescent species such as GDs are already determined, we can estimate I_0 and I_{90} for the film. Here, we denote the transition moments for the absorption and fluorescence of a fluorescent species as μ_A and μ_F , respectively. Let us imagine that all the chromophores, such as GDs, being isolated from each other, have the same arrangement in a film and their molecular motions are restricted perfectly. We define the angle between μ_A of the chromophore and Iv of the excitation light to be α (degree) and the angle between μ_F and Iv [of polarizer 2 (fluorescence)] to be β (degree). If a chromophore is excited at a wavelength of the first

absorption band according to the transition to the lowest excited state, namely, from S_0 to S_1 , β is identical to α . However, we can change μ_A , namely α , by shortening the wavelength. In this case, the intensity needed for a chromophore in the film to absorb the excitation light, shown as Iv , is proportional to $\cos^2 \alpha$, whereas the possibility of the polarized fluorescence of the chromophore passing through polarizer 2 is proportional to $\cos^2 \beta$. Thus, the intensity of I_0 monitored by the detector at the back of polarizer 2 is given by eq 1.

$$I_0 = K\Phi \cos^2 \alpha \cos^2 \beta \quad (1)$$

where K is the maximum probability of excitation attainable when the molecular axis of the chromophore coincides with the direction of Iv of the excitation light and Φ is the energy yield of fluorescence. I_{90} is obtained for the polarized fluorescence passing through polarizer 2 when it is set as Ih , namely, perpendicular to the case for I_0 . The angle between μ_F and Ih [of polarizer 2 (fluorescence)] is $90 - \beta$ (degrees), in which case I_{90} is given by eq 2.

$$I_{90} = K\Phi \cos^2 \alpha \sin^2 \beta \quad (2)$$

We can know the transition moments for the absorption and fluorescence of a chromophore, μ_A and μ_F , respectively. However, α and β are dependent on the three-dimensional position of the chromophore against Iv and Ih . Thus, it is obvious that the measurement of I_0 and I_{90} for one position is not enough for determining the arrangement of the chromophore, even if the arrangement of all the chromophores is unique.

Nishijima et al.³³ introduced a smart method for determining the position of chromophores in a film. In this method, each I_0 and I_{90} of the chromophore is measured by rotating the sample film around the excitation light beam in 10° increments or some other set number of degrees. This rotation increases the amount of information obtained about the arrangement of the chromophores in a film. Because the angles between the transition moments (μ_A and μ_F) and the three vectors of the electric field (Iv of the excitation and Iv and Ih of the fluorescence) must change, we can obtain the precise three-dimensional arrangement of chromophores at each rotation position. Accordingly, these three vectors of the electric field can be used as the standard coordinates.

Thus, if we can determine the three-dimensional arrangement of a guest chromophore in a film, we can calculate I_0 and I_{90} of the chromophore no matter how the film is positioned around the excitation light. Or, if the arrangement of a guest molecule is unique, we can estimate the arrangement by reproducing all the I_0 and I_{90} values obtained by rotating the sample.

RESULTS AND DISCUSSION

Thermal and Fluorescent Behaviors of PET Films As Received.

The WAXD pattern of PET film as received by a hot-pressed method (Figure 3) shows only Debye–Scherrer rings corresponding to the amorphous phase, indicating the

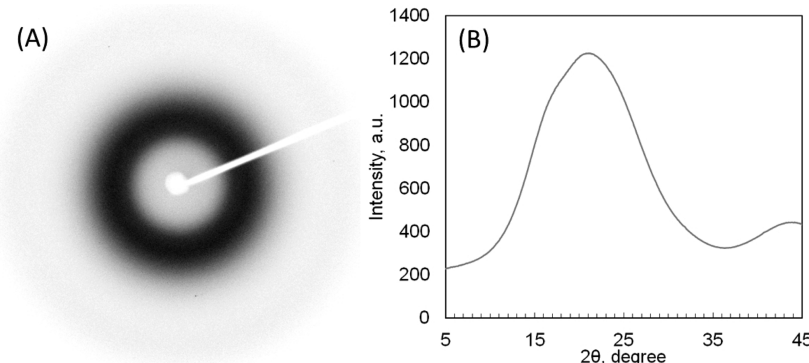


Figure 3. (A) X-ray diffraction pattern ($\text{Cu K}\alpha$) of nonstretched PET film and (B) the digital reading of the diffraction intensities at constant 2θ of (A) obtained by the integration of all the diffraction intensities around the beam. The maximum intensity appeared at 21.1° .

absence of either crystalline phase or any orientation of polymer chains in the film plane.

Figure 4 shows a DSC curve for the heating process of a hot-pressed PET film as received: all the PET films were prepared

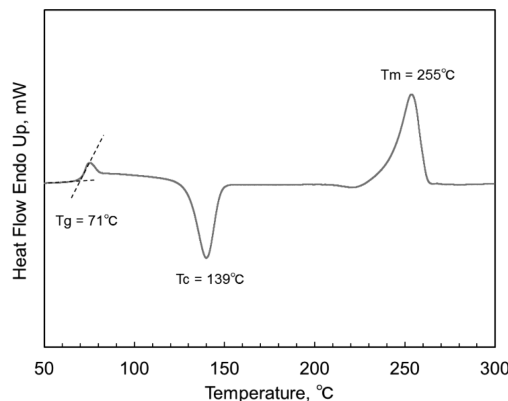


Figure 4. DSC heating curve for a PET film as received and used in the present work. Scan rate was $10\text{ }^{\circ}\text{C min}^{-1}$.

in the same way shown as in the Experimental Section. The peak temperature of the endothermic areas due to the melting was $255\text{ }^{\circ}\text{C}$, while the exothermic area due to cold crystallization, whose peak was $139\text{ }^{\circ}\text{C}$, began at $117\text{ }^{\circ}\text{C}$ and ended at $151\text{ }^{\circ}\text{C}$. The onset due to the glass transition was observed at $71\text{ }^{\circ}\text{C}$ while the transition ended at $80\text{ }^{\circ}\text{C}$.

Figure 5 shows the fluorescence spectrum of a PET film as received when it was excited at 340 nm . The fluorescence

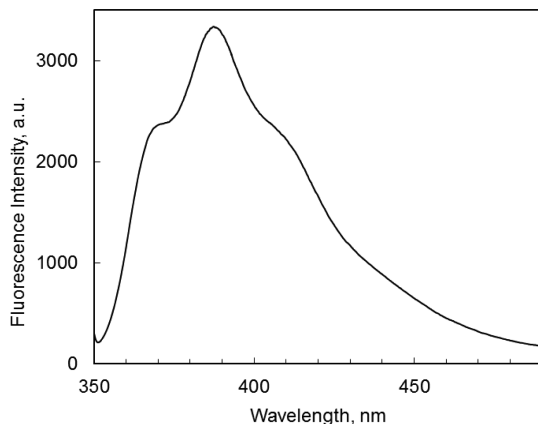


Figure 5. Fluorescence spectrum of GD of a PET film as received. Excitation wavelength was 340 nm . The film thickness was $236\text{ }\mu\text{m}$.

whose peak is at 390 nm has been reported as a ground-state dimer (GD) of PET.^{21–23} GD fluorescence of PET films is not observable for thin films prepared by using the spin-casting method.^{24,25,27} However, it can be observed for thick films such as PET bottles, as shown in Figure 5. The GD of a PET film is formed between two phenylene moieties whose π electrons overlap with each other. It is necessary that the two phenylene groups be within 0.35 nm of each other in order for them to interact. Many pairs of phenylene groups are assumed to interact with one another, but only pairs exhibiting this strict arrangement can form a GD. This is why thin PET films do not exhibit GD fluorescence; thus, the number of such exactly arranged pairs should be low.^{24,25} Note that a GD is formed only in the amorphous region of a PET film where it is possible

for a pair of phenylene rings to be located within 0.35 nm of each other. In the crystalline phase, it is impossible for any two phenylene groups to interact with each other. Because of the close packing of the crystalline molecules, the phenylene rings of neighboring PET chains slip past each other and are separated by more than 0.4 nm ; the crystalline form is triclinic ($a = 0.456\text{ nm}$; $b = 0.594\text{ nm}$; $c = 1.075\text{ nm}$; $\alpha = 98^{\circ}$; $\beta = 118^{\circ}$; $\gamma = 112^{\circ}$).¹⁰ Thus, the information obtained from GD fluorescence should reflect either the microenvironment in the amorphous phase or the onset mesomorphic mechanism of PET molecules.

Figure 6 shows the angular distributions of the polarized GD fluorescence intensities (I_{10} and I_{190}), namely PFR charts, of

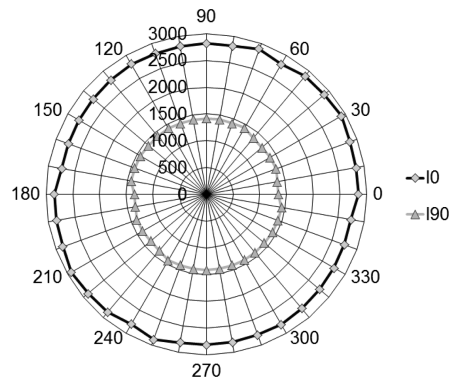


Figure 6. Angular distributions of I_{10} (◆) and I_{190} (▲) of GD fluorescence of nonstretched PET film: excitation wavelength is 340 nm . The numbers around the outer circle show the angles of setting a film from 0 to 360° ($=0^{\circ}$), while the distance from the center of the circle shows the intensity of polarized fluorescence I_{10} and I_{190} .

unstretched PET film in the circular polar coordinate, which is convenient to survey the changes of I_{10} and I_{190} with a rotation angle. The numbers around the outer circle show the angles of setting a film from 0 to 360° ($=0^{\circ}$), while the distance from the center of the circle shows the intensity of polarized fluorescence (I_{10} and I_{190}). The PFR chart as a symmetric circle demonstrates that the GDs are distributed uniformly and isotropically all over the film. Because GD is formed only in the amorphous region, the isotropic distributions of I_{10} and I_{190} mean that PET chains are not oriented at all in the amorphous region of unstretched PET films.

Orientation of GD in Uniaxially Stretched PET Films. We examined the effect of drawing temperatures lower or higher than T_g . Figure 7A1 shows the WAXD pattern of a uniaxially stretched PET film with a drawing ratio of 4.0 at $67\text{ }^{\circ}\text{C}$ (lower than T_g), showing a broad peak on the equator. The figure clearly demonstrates that PET chains in the amorphous region are highly oriented along the drawing direction. On the meridian, a weak but sharp peak appeared, having a spacing of 1.04 nm ($2\theta \approx 8.6^{\circ}$). The meridional reflection was already reported by Asano et al. as being due to a mesomorphic ordering.¹¹ Figure 7A2 is the WAXD pattern of PET drawn at $80\text{ }^{\circ}\text{C}$ (higher than T_g). The amorphous scattering is spread around the equator, showing low orientation due to relaxation of the drawn polymer molecules. Figure 7A2 does not show any peak on the meridian.

The PFR results are shown in Figure 7B. The angular distributions of I_{10} and I_{190} had peaks at 90° and 270° for I_{10} and at 45° , 135° , 225° , and 315° for I_{190} . The distribution patterns provide information on the orientation direction of chromo-

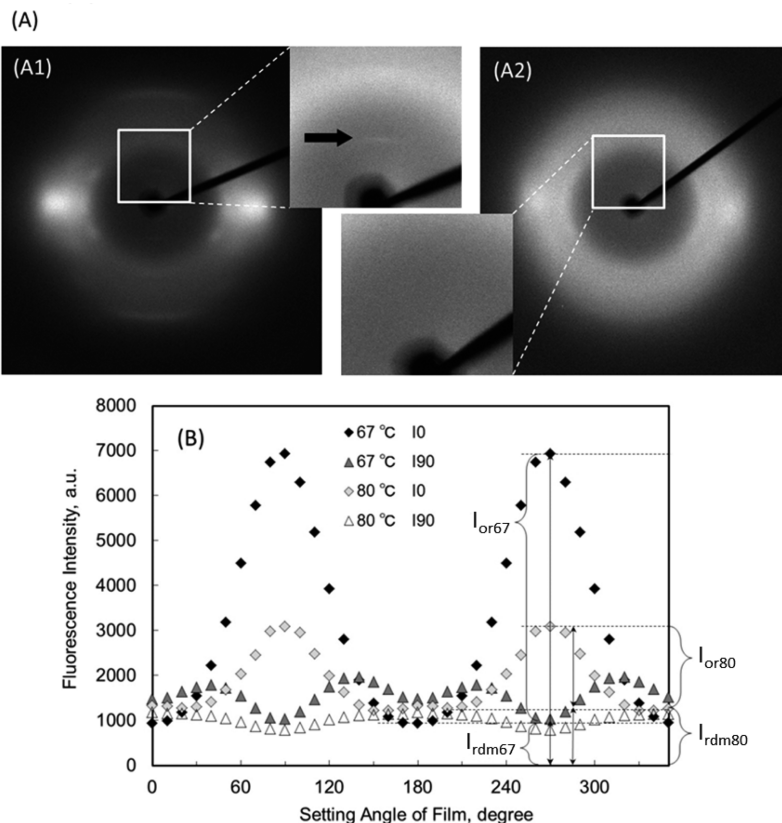


Figure 7. (A) X-ray diffraction patterns of uniaxially stretched PET films ($\lambda \approx 4$). The drawing temperature was (A1) 67 °C and (A2) 80 °C (T_g of the unstretched PET film was 71 °C). (B) Angular distributions of I_0 (◆) and I_{90} (▲) of the GD of a uniaxially stretched PET film; excitation wavelength is 340 nm. The detector voltage was higher than that used for Figures 5 and 6 because the drawn films were thinner and had smaller values of I_0 and I_{90} under the same conditions as the measurements.

phores.³¹ We have attempted to analyze the orientation of mesomorphic ordering in detail, although it is still an open problem. From these PFR charts, it is obvious that the main chain of PET in the amorphous region is oriented toward a specific direction by uniaxial stretching without crystallization because GDs are present only in the amorphous region. In particular, PFR charts can provide us with quantitative information about the relative fractions of the oriented and unoriented regions.

We would like to explain the change in the orientation fraction of PET chains when the films were drawn at 67 and 80 °C by using I_0 values. Here, we define the fluorescence intensity of GDs in the oriented and unoriented regions as I_{or} and I_{rdm} , respectively. I_{rdm} is a constant value that does not change with the setting film angle. On the other hand, I_{or} changes with the setting film angle, and its minimum value is considered to be 0. Here, we define the orientation degree, OD, as

$$\text{OD} = I_{\text{or}} / (I_{\text{or}} + I_{\text{rdm}}) \quad (3)$$

As for I_0 of the drawn PET at 67 °C shown in Figure 7B, the fluorescence intensities of GDs that are distributed at random, $I_{\text{rdm}67}$, and those that are highly oriented toward some direction, $I_{\text{or}67}$, can be discerned from the angular distributions of I_0 , as shown in Figure 7B. In the case of I_0 of the drawn PET at 67 °C, $I_{\text{rdm}67}$, namely, the valley value of periodical changes, is ~950, whereas the maximum value of I_0 is ~6940. Thus, the OD can be estimated to be about 0.86 [(6940 – 950)/6940]. Meanwhile, in the case of I_0 of the drawn PET at 80 °C, the

minimum and maximum values are ~1230 and ~3100, respectively. Therefore, its OD was estimated to be about 0.60 [(3100 – 1230)/3100]. Note that this OD value is not the absolute fraction of the oriented order because I_0 and I_{90} values in the oriented and unoriented regions are dependent not only on the number of molecules but also on the machine constant. For example, as with the calculation of I_0 , the estimated values of OD calculated from I_{90} are 0.47 [(1980 – 1040)/1980] for 67 °C and 0.33 [(1190 – 800)/1190] for 80 °C. Although the apparent values are different, the change of OD values obtained from I_0 is from 0.86 to 0.60, whereas the change obtained from I_{90} is from 0.47 to 0.33. Thus, the change of OD values between 67 and 80 °C is found to be exactly the same: 0.70 (0.60/0.86) calculated from I_0 and 0.70 (0.33/0.47) calculated from I_{90} .³⁴ This change means the orientation degrees of the PET films drawn at 80 °C decreased to 70% that of the films drawn at 67 °C.

These results show that PFR is a convenient way of estimating the fractions of the oriented and unoriented regions in polymer films, the same as some XRD methods.³⁵ The PFR results shown in Figure 7B were consistent with the WAXD observations of Figure 7A. Thus, the feasibility of using PFR to check the number of GDs and mesomorphic ordering is demonstrated.

Triclinic Crystallization of the Uniaxially Stretched PET Films by Annealing at Temperatures over T_c . We have studied the triclinic crystallization process of PET by comparison of PFR and WAXD results. PET films drawn at 67

°C were annealed for 24 h under vacuum at some higher temperatures than T_c (139 °C as shown in Figure 4).

Figure 8 shows WAXD patterns drawn at 67 °C and then annealed at 140 and 200 °C. The triclinic reflections are sharper

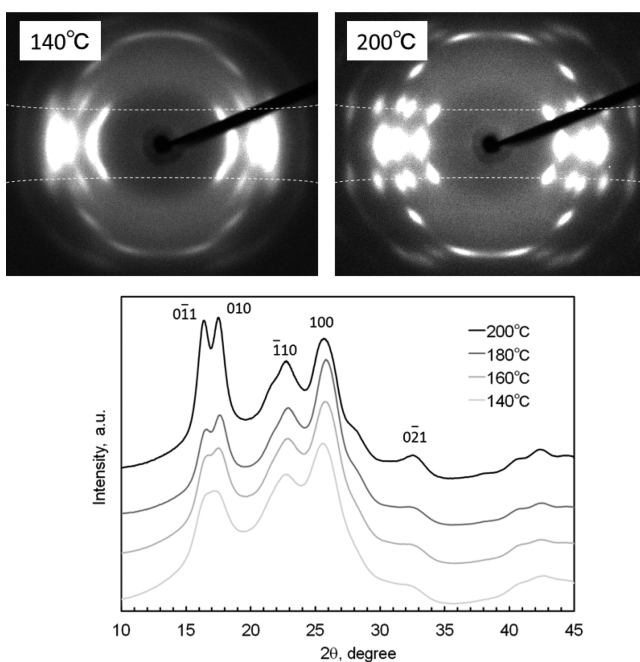


Figure 8. WAXD patterns of PET films drawn at 67 °C ($\lambda \approx 4$) and then annealed for 24 h at different temperatures from 140 to 200 °C. The dotted lines in 2D images (upper pictures) show the first layer lines.

at 200 °C, indicating that the oriented triclinic crystal is developed with an increase of annealing temperature.^{11,14} The parabolic first layer lines are shown in the WAXD patterns. Note that the triclinic reflections on the first layer (hkl) are displaced up and down from the layer positions. This is due to a unique tilted orientation which appeared in oriented PET films.^{7,10,11} Asano and Seto have already discussed the mechanism of the tilted orientation.¹¹ Because of the density difference of the amorphous and crystalline layers, the alternative crystalline and amorphous layers are inclined oppositely; hence, the triclinic *c*-axis is tilted in the special

manner depending on the annealing temperature. The mechanism is closely related to the process of crystallization such as precursor structure including the mesomorphic state. The example of the initial crystallization process around T_g will be explained in the final section.

Next we measured the PFR of these PET films that were uniaxially drawn at 67 °C and annealed for 24 h at several temperatures. The annealing temperature dependence of PFR shown in Figure 9 can be summarized as follows: (1) the patterns of angular distributions of I0 and I90 for drawn PET films are similar to those shown in Figure 7B: all the maximum values of I0 appear at 90° and 270°, while all the maximum values of I90 appear at 45°, 135°, 225°, and 315°; however, (2) all the values of I0 and I90 at any setting angle of films decreased with an increase in annealing temperature in spite of the similar shape of the angular distributions.

In general, a GD is formed between two phenylene rings by being in contact with both π -electron orbitals together. Thus, the presence of GDs in the present PET systems means that a phenylene group of a PET chain contacts with another phenylene group of another PET chain, indicating that GD fluorescence comes out of a phenylene group in the amorphous region because any phenylene moieties are separated from each other in the crystalline phase. In conclusion, the PFR results of the GD fluorescence of PET show the amount and orientation of the amorphous region. As explained in the section on PFR, we can calculate the distribution of phenylene groups in more detail using eqs 1 and 2 if the transition moments for absorption, μ_A , and fluorescence, μ_F , of a PET GD are already established. However, even the arrangement of two benzene rings in benzene dimers has not been determined yet.³⁶

The maximum I0 appears at 90° and 270°, and the maximum I90 appears at 45°, 135°, 225°, and 315°. These angles are considered to show the directions in which PET main chains are parallel to each other, regardless of the transition moments showing absorption and fluorescence of a PET GD.³⁷ In any case, cold crystallization proceeds with an increase in annealing temperature over T_c , and the fraction of the amorphous region decreases with an increase in the fraction of the triclinic crystalline phase of PET. The PFR measurements shown in Figure 9 were carried out for films with a thickness of ~100 μm annealed at different temperatures. Thus, this decrease of I0 and I90 indicates that the crystallization takes place along with

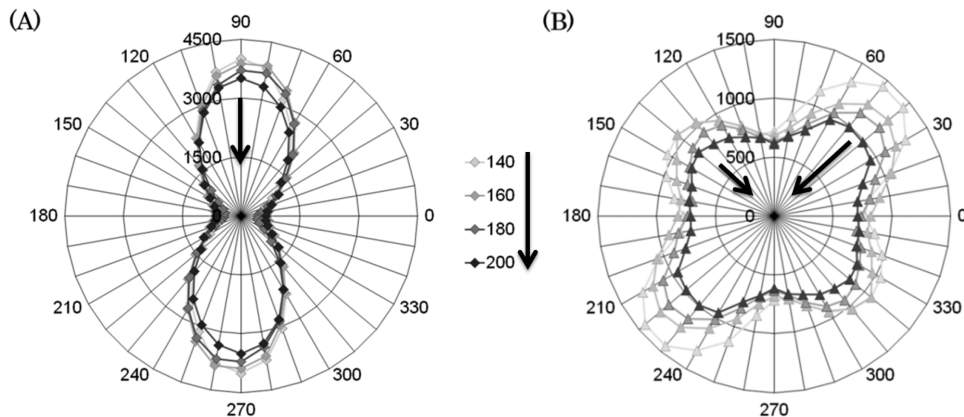


Figure 9. Angular distributions of (A) I0 and (B) I90 of PET GD films that were stretched uniaxially at 67 °C and annealed for 24 h at different temperatures over T_c . The same drawn PET film was fixed with a metallic binder and annealed at different temperatures. The excitation wavelength was 340 nm.

the orientation of PET main chains induced by the stretching. As described in "Orientation of GD in Uniaxially Stretched PET Films", the PFR charts can give quantitative information about the fractions of the oriented and unoriented regions. Since the relative fraction of oriented region is expressed by OD value (eq 3), we can compare the fraction values with an increase in annealing temperature. In the case of I90, the OD values were 0.509 (annealed at 140 °C), 0.461 (at 160 °C), 0.458 (at 180 °C), and 0.382 (at 200 °C), meaning that the fraction of the unoriented region, 1-OD, were 0.491 (at 140 °C), 0.539 (at 160 °C), 0.542 (at 180 °C), and 0.618 (at 200 °C). The change of the OD values means that the crystallization of drawn PET films take place more favorable in the oriented region. Here it is to be emphasized that the I0 and I90 of GD in PET films must decrease with a progress of cold crystallization process that is promoted at higher temperatures.

Initial Process of Structural Changes Induced by Annealing around T_g .

Figure 10 shows WAXD patterns of

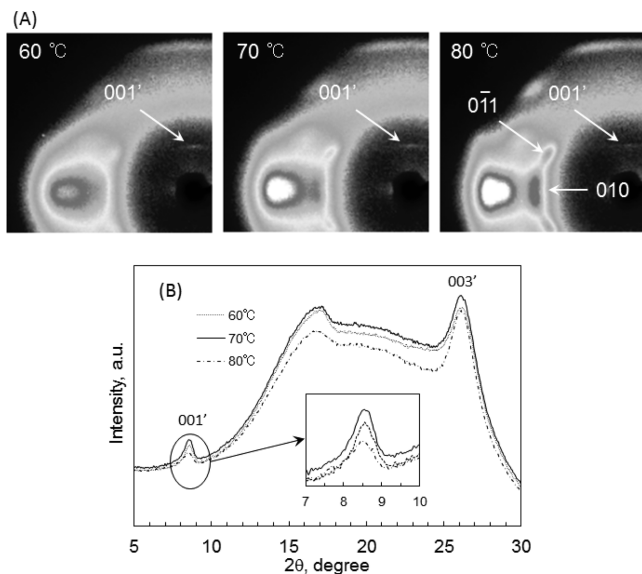


Figure 10. X-ray diffraction patterns of uniaxially stretched PET films ($\lambda \approx 4$) at 67 °C after they were annealed for 24 h around T_g . (A) 2D images: a signal corresponding to 001' appeared on the meridional line, and 010 and 011 reflections clearly appeared at 80 °C. (B) Integration of signal intensities only toward the meridional line.

PET drawn at 67 °C and annealed at 60, 70, and 80 °C for 24 h. All the measurements were carried out on different pieces of the same drawn film. These pieces were fixed with a metallic binder and annealed at each temperature. After annealing at one temperature, a piece of the film was cut and measured with WAXD and PFR. The rest of the film was again fixed with a binder and annealed at the next higher temperature. The thickness of each film was approximately $103 \pm 3 \mu\text{m}$. The patterns indicate that (1) there are no sharp triclinic peaks as are shown in Figure 8, (2) some preliminary changes appear in the amorphous region, indicating the presence of mesomorphic ordering, and (3) there is a weak but sharp reflection on the meridian. The spacing of the meridional peak is $d \approx 1.04 \text{ nm}$ ($2\theta \approx 8.6^\circ$).

Asano et al. reported the emergence of the meridional peak in the preliminary stage and assigned it as being from a paracrystalline or smectic structure.^{13,14} The present results also

confirm the presence of mesomorphic ordering. The integrated intensity of the meridional peak was counted by the software of the X-ray apparatus, and the results are summarized as a function of the annealing temperature in Figure 10B. Sharp reflections of 001' and 003' are clearly observed and show high coherency of the mesomorphic state. Thus, we judge that the smectic form is established by the annealing of drawn PET films at a temperature around T_g .

Figure 11 shows the PFR chart, i.e., the angular distributions of I0 and I90 of the GDs of the same PET films used for the WAXD measurements of Figure 10. The distribution patterns are similar to those of Figure 9, where I0 has peaks at 90° and 270° and I90 has peaks at 45°, 135°, 225°, and 315°. However, there is a remarkable difference in the annealing temperature dependence. In the case of the films annealed at temperatures higher than 140 °C, a PET triclinic crystalline phase was formed. Then, the polarized fluorescence intensities, I0 and I90, of the GD decreased with increasing temperatures (Figure 9). On the other hand, for PET films annealed at low temperatures (Figure 11), the distribution patterns of I0 and I90 were found to show different features with an increase in annealing temperature. Because the thicknesses of the films were almost the same as that described above (approximately $103 \pm 3 \mu\text{m}$), there is no question that I0 and I90 reached their maximum values at an annealing temperature of 70 °C.

In order to examine the annealing temperature dependence of I0 and I90 in more detail, we set a stretched PET film on an aluminum plate and annealed it together with the plate. In this case, we were able to repeatedly measure the fluorescence intensity of the same area of the same film with high accuracy and high reproducibility. We measured I0 of the GD with the angle of the film fixed at 90°, which is the peak for I0 in all of the setting angles of the film. Figure 12 shows the dependence of I0 of the GD on the annealing temperature, together with the X-ray reflection intensity of the peak corresponding to the smectic ordering (001'). The maximum I0 value appeared at 65 °C, where the intensity of the meridional reflection also had a maximum at 70 °C. It is interesting that the annealing temperature at which the GD fluorescence showed the highest intensity nearly coincided with that at which the WAXD peak corresponding to the smectic reflection showed the highest intensity. Thus, the results shown in Figure 12 indicate important evidence that the GD formation in the oriented amorphous region was strongly related to the formation of the mesomorphic order, which was assigned to smectic ordering.

The drawing of a PET film is assumed to compel the orientation of each PET chain to be parallel to the drawing direction, but the arrangement of each main-chain phenylene group is not perfectly parallel, as shown in Figure 13A. In the case of the GD of PET, the value of I0 for GD takes its maximum value when the setting angle of the drawn PET film is 90° (Figure 7). This means that the I0 of GD has its maximum value when the drawing direction of the PET film is parallel to Iv in Figure 1. Figure 13B demonstrates the concept of smectic ordering. Large-scale motion of the main chains is restricted at temperatures around T_g , although many PET chains in the drawn film can be aligned to be parallel to each other. The smectic structure needs to be advantageous in terms of energy as a metastable structure. Therefore, it is possible to consider that the GD has an important role to play in the formation of smectic ordering. Annealing at this low temperature is considered to enable rotation of ethylene parts and phenylene parts of PET around the main chain. Rotation of an

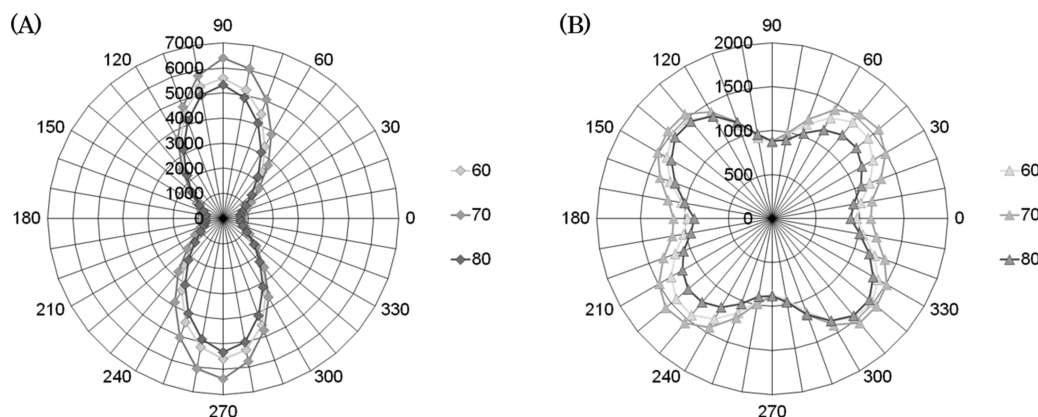


Figure 11. Angular distributions of (A) I0 and (B) I90 of GD of PET films that were uniaxially stretched at 67 °C and annealed for 24 h at some temperatures around T_g ; excitation wavelength is 340 nm. All the PFR and WAXD results shown in Figures 10 and 11 were carried out for the same film. In order to make sure, the voltage of the detector was increased, so the values of I0 and I90 were not compared with those of Figure 9. The maximum intensities of I0 and I90 were of the order with 70 °C > 60 °C > 80 °C.

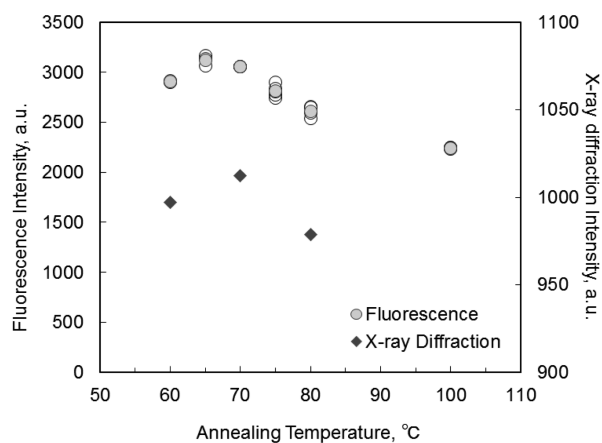


Figure 12. Annealing temperature dependence of I0 for GD and the WAXD intensity of mesomorphic structure corresponding to 001' reflection, which is assigned to smectic ordering, of a PET film stretched uniaxially at 67 °C. Each I0 value was obtained by setting the film angle to be 90°: the stretching direction is 0°. The area of the film excited by light (340 nm) was all the same. The annealing time at each temperature is 24 h. The open and gray circles mean experimental values and their averages at each temperature, respectively.

ethylene part could either lengthen or shorten the linear portion of the PET chain, so the annealing process sometimes causes two phenylene groups of different PET chains to come into contact with each other. On the other hand, rotation of a phenylene part can orientate two phenylene groups that are close to each other such that they are parallel. Thus, annealing at low temperatures appears to increase the possibility that two phenylene groups on different chains could come into contact with each other and their orientations could become parallel to each other. In this case, if two phenylene groups, which are of planar structures, are in a parallel orientation, the $\pi-\pi$ interaction between the two flat phenylene rings makes them form a GD. This is the reason why the fluorescence intensity of GD increases when PET films are annealed at temperatures around T_g .

Figures 10, 11, and 12 have clearly proved that the formation and growth of the mesomorphic structure, whose presence can be monitored by the 001' reflection, is closely related to the formation of phenylene GDs, even if this mesomorphic structure is not of exact smectic ordering but rather partially consists of random sequences of monomeric units in different minimum-energy conformations.^{12,13}

So far, we have explained that the increase in GD formation induced by annealing at low temperatures around T_g is strongly related to the formation of a mesomorphic structure, which is

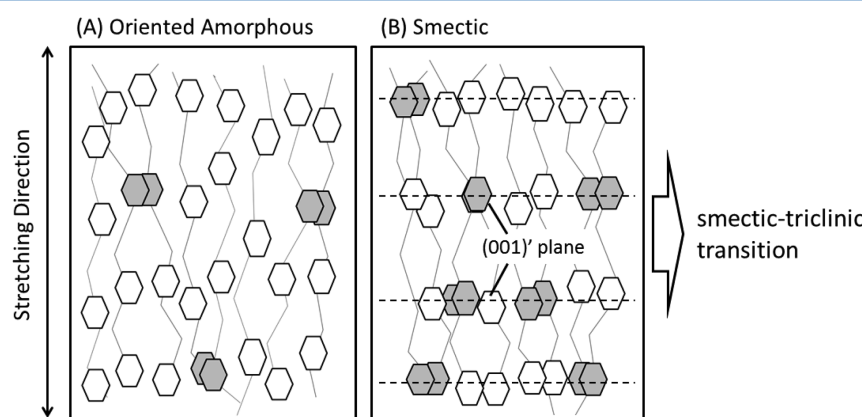


Figure 13. Sketch of the distributions of main-chain phenylene rings of PET chain: (A) uniaxially stretched film without annealing and (B) the same film showing (001)' plane after being annealed around 70 °C.

assigned to the smectic ordering of PET chains on the basis of Figure 10B. The formation of a GD is mainly due to π - π interactions between two flat phenylene rings. Taking into account all of the data shown above, we speculate that the π - π interaction between main-chain phenylene groups is the main factor in producing smectic ordering by annealing at around 60–70 °C. The formation of the smectic ordering has already been demonstrated by means of synchrotron wide-angle X-ray diffraction^{15,16} of transient structures in cold-drawn PET fibers to be quite rapid. We have already shown that phenylene groups of PET main chains in amorphous regions interact with each other due to the π - π interactions between two flat phenylene groups. The phenylene fluorescence of PET is shifted to the red in comparison with the normal fluorescence of isolated phenylene groups.^{24,25} A GD, which has a strict and stable arrangement of two phenylene groups even in the ground state, is just one of the phenylene pairs that interact with one another. When the fluorescence of a GD is observable, many phenylene groups are concluded to overlap with each other.

Considering the rapid development of the smectic ordering at low temperature,^{15,16} the GD seems to connect the neighboring nematic chains at the same level, thus producing a smectic order. Thus, we assume that GDs serve as nucleation centers in the formation process of the smectic ordering. Because of the formation of GDs, the main-chain phenylene rings of the neighboring PET chains are aligned on the 001' smectic plane, as shown in Figure 13B.

The neutral benzene dimer in the gas phase has been studied experimentally^{38,39} and theoretically.^{36,40} The binding energies of the benzene dimer were obtained by indirect measurements from the dissociation energy of the cation and the ionization potentials of the dimer and monomer: the values are 1.6³⁹ and 2.4 kcal/mol.³⁸ The values of the binding energy calculated theoretically are mostly in the range between 2 and 4 kcal/mol.^{36,40} In the case of phenol (i.e., a monosubstituted benzene) the antiparallel-displaced form is calculated to be more stable as a dimer than the parallel-displaced form: the former is 4.2 kcal/mol whereas the latter is 3.0 kcal/mol.⁴¹ These values of binding energy are reasonable for the GD of PET to act as a nucleation center. Thus, our idea that the formation of GD by π - π interactions that then stimulates smectic ordering is reasonable.

Influence of the Smectic Ordering on the Tilt Orientation. We have demonstrated that the formation of GDs is strongly related to the formation of smectic ordering during the annealing of PET films at temperatures around T_g . We would like to suggest in this section that smectic ordering induces the tilt orientation of the PET crystalline form during the smectic–triclinic transition.

In Figure 10, the equatorial reflection changed with the annealing temperature, showing the transition from smectic to triclinic. The 010 reflection developed in the following way: diffuse scattering at 60 °C, weak reflection on the equator at 70 °C, and stronger reflection streaked up and down from the equator at 80 °C. The streak was spread $\pm 10^\circ$ from the equator. Choosing the middle of the streak, the triclinic (010) plane was measured to incline from the equator by approximately 5°. On the first layer line, the intensity of the 01 reflection became stronger than the other reflections. The position of 01 appeared lower than the normal layer line. These results indicate that triclinic ordering preferentially developed along the b -axis at 80 °C.

Let us consider here the section of the bc -plane of the triclinic PET. In Figure 14A, the c -axis is parallel to the draw

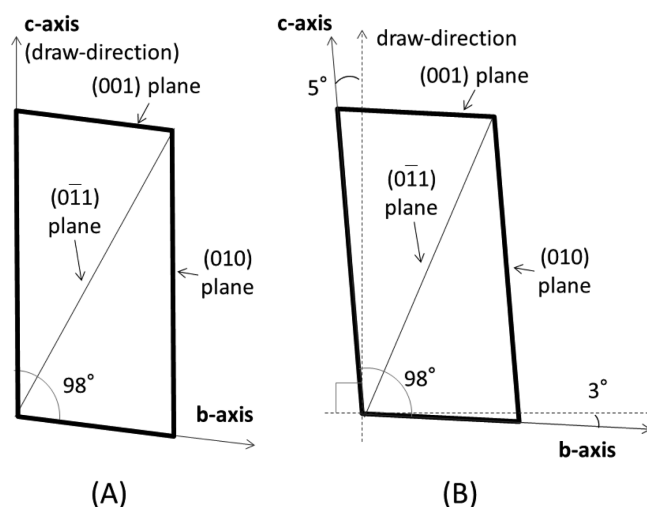


Figure 14. A section of the bc -plane of the triclinic PET crystal. The angle between the c -axis and the b -axis is 98° .¹⁰ (A) The c -axis is parallel to the draw direction. (B) The c -axis is tilted 5° in an anticlockwise direction.

direction. On the other hand, the c -axis is tilted 5° in an anticlockwise direction in Figure 14B. By the tilting, the 010 reflection shifts upward from the equator and the 011 reflection shifts downward from the first layer line, which well fits with the results shown in Figure 10.

The neighboring phenylene rings are arranged parallel to the (001)' plane in the smectic state, while they are parallel to the (001) plane in the triclinic crystal. Because of the tilting by 5°, the inclination of the (001) plane is reduced to 3°, as shown in Figure 15B. During the smectic–triclinic transition at low

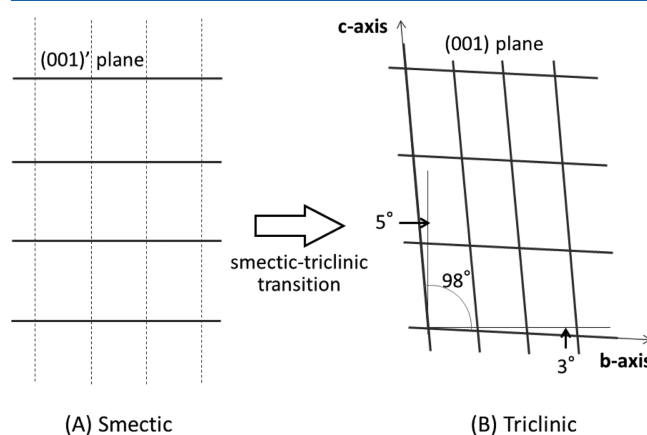


Figure 15. Comparison of the inclination of the smectic (001)' plane and the triclinic (001) plane. Because of the tilting of the triclinic c -axis, the difference is reduced to 3°.

temperature, it is difficult to significantly shift the phenylene positions along the PET chain. Thus, the tilting makes it easier to reduce the displacement. As a result, we can conclude that the smectic ordering induces the tilt orientation of the triclinic PET during the smectic–triclinic transition. The WAXD results shown in Figure 10 will agree with the crystallization of the cold-drawn PET.^{11,14}

Comparing the results of PFR and WAXD, it is possible to conclude that the GDs are aligned on a flat plane, introducing smectic ordering during crystallization around T_g . At higher temperatures, a triclinic crystal structure showing a unique tilted orientation develops from the smectic state. In this process, the triclinic (001) plane is nearly parallel to the smectic (001)' plane. The present result strongly implies that the smectic order and subsequent tilted orientation originated either from the GDs or from the π - π interaction between the main-chain phenylene groups.

AUTHOR INFORMATION

Corresponding Author

*Tel +81-54-238-4627, Fax +81-54-237-3354, e-mail edhitag@ipc.shizuoka.ac.jp (H.I.).

Notes

The authors declare no competing financial interest.

ACKNOWLEDGMENTS

This work was supported by Grant-in-aid for Scientific Research (C) (21550206) from the Ministry of Education, Science, Sports and Culture of Japan. The authors are grateful to Sho Kurihara and Yumi Takahama of Shizuoka University for their measurements. The research was partially carried out at the Center for the Instrumental Analysis, Shizuoka University.

ABBREVIATIONS

PET, poly(ethylene terephthalate); WAXD, wide-angle X-ray diffraction; PFR, the method of measuring polarized fluorescence intensities by rotating a sample around the excitation light; GD, ground-state dimer.

REFERENCES

- (1) Keller, A.; Lester, G. R.; Morgan, L. B.; Hartley, F. D.; Lord, E. W. *Philos. Trans. R. Soc.* **1954**, A-1 (247), 13.
- (2) Zachmann, H. G.; Stuart, H. A. *Makromol. Chem.* **1960**, *41*, 131.
- (3) Elsner, G.; Koch, M. H. J.; Bordas, J.; Zachmann, H. G. *Makromol. Chem.* **1981**, *181*, 1263.
- (4) Elsner, G.; Rickel, C.; Zachmann, H. G. *Adv. Polym. Sci.* **1985**, *67*, 1.
- (5) Günter, B.; Zachmann, H. G. *Polymer* **1983**, *24*, 1008.
- (6) Asano, T.; Zdeick-Pickuth, A.; Zachmann, H. G. *J. Mater. Sci.* **1989**, *24*, 1967.
- (7) Bonart, R. *Kolloid-Z.* **1964**, *199*, 136.
- (8) Yeh, G. S. Y.; Geil, P. H. *J. Macromol. Sci., Part B* **1967**, *1*, 235.
- (9) Yeh, G. S. Y.; Geil, P. H. *J. Macromol. Sci., Part B* **1967**, *1*, 251.
- (10) Daubeny, R.; de, P.; Bunn, C. W.; Brown, C. J. *Proc. R. Soc., Ser. A* **1954**, *226*, 531–542.
- (11) Asano, T.; Seto, T. *Polym. J.* **1973**, *5*, 72–85.
- (12) Auriemma, F.; Corradini, P.; De Rosa, C.; Guerra, G.; Petraccone, V.; Bianchi, R.; Di Dino, G. *Macromolecules* **1992**, *25*, 2490–2497.
- (13) Parravicini, L.; Leone, B.; Auriemma, F.; Guerra, G.; Petraccone, V.; Di Dino, G.; Bianchi, R.; Vosa, R. *J. Appl. Polym. Sci.* **1994**, *52*, 875–885.
- (14) Asano, T.; Baltá Calleja, F. J.; Flores, A.; Tanigaki, M.; Mina, F.; Sawatari, C.; Itagaki, H.; Takahashi, H.; Hatta, I. *Polymer* **1999**, *40*, 6475–6484.
- (15) Keum, J. K.; Kim, J.; Lee, S. M.; Song, H. H.; Son, Y.-K.; Choi, J.-I.; Im, S. S. *Macromolecules* **2003**, *36*, 9873–9878.
- (16) Kim, K.-H.; Murata, T.; Kang, Y.-A.; Ohkoshi, Y.; Gotoh, Y.; Nagura, M.; Urakawa, H. *Macromolecules* **2011**, *44*, 7378–7384.
- (17) Yamaguchi, T.; Kim, K.; Murata, T.; Koide, M.; Hitoosa, S.; Urakawa, H.; Ohkoshi, Y.; Gotoh, Y.; Nagura, M.; Kotera, M.; Kajiwara, K. *J. Polym. Sci., Part B: Polym. Phys.* **2008**, *46*, 2126–2142.
- (18) Kawakami, D.; Hsiao, B. S.; Burger, C.; Ran, S.; Avila-Orta, C.; Sics, I.; Kikutani, T.; Jacob, K. I.; Chu, B. *Macromolecules* **2005**, *38*, 91–103.
- (19) Mahendrasingam, A.; Blundell, D. J.; Wright, A. K.; Urban, V.; Narayanan, T.; Fuller, W. *Polymer* **2003**, *44*, 5915–5925.
- (20) Mahendrasingam, A.; Blundell, D. J.; Martin, C.; Urban, V.; Narayanan, T.; Fuller, W. *Polymer* **2005**, *46*, 6044–6049.
- (21) Hennecke, M.; Kud, A.; Kurz, K.; Fuhrmann, J. *Colloid Polym. Sci.* **1987**, *265*, 674–680.
- (22) Hemker, D. J.; Frank, C. W. *Polymer* **1988**, *29*, 437–447.
- (23) Sonnenschein, M. F.; Rpland, C. M. *Polymer* **1990**, *31*, 2023–2026.
- (24) Itagaki, H.; Inagaki, Y.; Kobayashi, N. *Polymer* **1996**, *37*, 3553–3558.
- (25) Itagaki, H. *J. Lumin.* **1997**, *72*–74, 435.
- (26) Itagaki, H.; Arakawa, S. *Polymer* **2003**, *44*, 3921–3926.
- (27) Itagaki, H.; Kato, S. *Polymer* **1999**, *40*, 3501–3504.
- (28) Itagaki, H.; Arakawa, S. *Polymer* **2009**, *50*, 1491–1496.
- (29) Itagaki, H.; Sago, T.; Uematsu, M.; Yoshioka, G.; Correa, A.; Venditto, V.; Guerra, G. *Macromolecules* **2008**, *41*, 9156–9164.
- (30) Sago, T.; Itagaki, H. *J. Photopolym. Sci. Technol.* **2010**, *23*, 357–362.
- (31) Sago, T.; Itagaki, H.; Asano, T. *Soft Mater.* **2011**, *9*, 199–223.
- (32) Sago, T.; Itagaki, H. *J. Photopolym. Sci. Technol.* **2011**, *24*, 349–355.
- (33) (a) Nishijima, Y.; Onogi, Y.; Asai, T. *J. Polym. Sci., Part C* **1967**, *15*, 237–250. (b) Nishijima, Y. *J. Polym. Sci., Part C* **1970**, *31*, 353–373.
- (34) We did not show the absolute value of orientation degree in the present paper. However, it is possible to determine it because the machine constant can be calculated by comparing the orientation degree obtained from PFR method with the Herman's orientation function obtained from WAXD analysis.
- (35) Wu, J.; Schultz, J. M. *Polymer* **2002**, *43*, 6695–6700.
- (36) Sinnokrot, M. O.; Sherrill, C. D. *J. Phys. Chem. A* **2006**, *110*, 10656–10668.
- (37) Several visualized models of PFR charts together with arrangement of a fluorescent molecule in a film are shown in detail in ref 31.
- (38) Grover, J. R.; Waiters, E. A.; Huit, E. T. *J. Phys. Chem.* **1987**, *91*, 3233–3237.
- (39) Krause, H.; Ernstberger, B.; Neusser, H. *J. Chem. Phys. Lett.* **1991**, *184*, 411–417.
- (40) Sinnokrot, M. O.; Valeev, E. F.; Sherrill, C. D. *J. Am. Chem. Soc.* **2002**, *124*, 10887–10893.
- (41) Seo, J.-I.; Kim, I.; Lee, Y. S. *Chem. Phys. Lett.* **2009**, *474*, 101–106.